ELSEVIER

Journal of Alloys and Compounds 465 (2008) 239–243

Journal of ALLOYS AND COMPOUNDS

www.elsevier.com/locate/jallcom

Pressureless infiltration of liquid aluminum alloy into SiC preforms to form near-net-shape SiC/Al composites

Junwu Liu, Zhixiang Zheng *, Jianmin Wang, Yucheng Wu, Wenming Tang, Jun Lü

School of Materials Science and Engineering, Hefei University of Technology, Tunxi Road 193, Hefei, Anhui 230009, PR China

Received 19 April 2007; received in revised form 11 October 2007; accepted 13 October 2007
Available online 22 October 2007

Abstract

SiC/Al composites with uniformly distributed SiC particles were fabricated by pressureless infiltration of liquid $AlSi_7Mg$ alloy into SiC preforms with different porosity derived from SiC powders. The linear expansion of SiC preforms without any deformation was about 4% due to the oxidation of SiC powders during the sintering process. SiC preforms had no change in both shape and dimensions after infiltration so that near-net-shape composites were achieved. As SiC volume fraction varies from 39% to 62%, the thermal conductivity of SiC/Al composites with bending strength beyond 360 MPa and elastic modulus beyond 140 GPa varies from 146 to 118 $W\,m^{-1}\,K^{-1}$ at room temperature, and the mean linear coefficient of thermal expansion from room temperature to 373 K varies from 10×10^{-6} to $7.69 \times 10^{-6}\,K^{-1}$, agreeing better with the Turner's model.

Keywords: Metal matrix composites; Mechanical properties; Thermal expansion; Pressureless infiltration; Near-net-shape

1. Introduction

SiC/Al composites with high SiC volume fraction have low coefficient of thermal expansion (CTE) and good thermal conductivity (TC). Comparing with W–Cu alloys, SiC/Al composites not only have higher specific strength and elastic modulus, but also have lower cost in raw materials, which made them more suitable for applications such as space structures and electronic heat sinks in motion vehicles [1–4]. High SiC volume fraction makes SiC/Al composites machined very difficultly owing to the abrasive resistance nature of SiC filler, so near-net-shape processes with little machining become the optimum candidates to lower production cost. The infiltration of liquid Aluminum alloy into SiC preforms with open pores is one of near-net-shape process accepted by most material researchers. Pressure infiltration routine has been successfully applied in industry by several companies [5–7]. Pressureless infiltration now attracts considerable attention in recently years as it avoids expansive mould bearing heat and pressure impact in pressure infiltration process which usually leads crazing of brittle SiC preforms [8–14].

Pressureless infiltration to near-net-shape routine includes two steps: the preparation of SiC preforms and liquid metal spontaneous penetrating into porous preforms to form SiC/Al composites [12,15]. It has significant sense to study the porosity and dimension change during the preparation of SiC preforms for structure–function integrative process because the aluminum alloy content in the composites lies on its porosity, the figuration and tolerance of the composites are both lie on the shape and dimension change of the preforms. Although SiC preforms for pressure infiltration has been investigated by several researchers [16,17], there are few reports on the preparation of SiC preforms for pressureless routine as the poor wettability between the SiC preforms and liquid aluminum alloy is the main barrier for spontaneous penetration.

In this paper, SiC/Al composites with near-net-shape and different filler volume fraction were manufactured by pressureless infiltration. SiC preforms with different porosity were manufactured by oxidation bonding process at low temperature in atmosphere. Spontaneous infiltration of liquid $AlSi_7Mg$ into the preforms were achieved by the assistance of interface reaction between liquid alloy containing magnesium and solid SiO_2 film in SiC preforms which leads to good wettability of the two phases. The dimension change of the samples in the whole

* Corresponding author at: School of Materials Science and Engineering, Hefei University of Technology, Tunxi Road 193, Hefei, Anhui 230009, PR China. Tel.: +86 551 2901372; fax: +86 551 2901362.
E-mail addresses: jwliu@hfut.edu.cn, jwliu12@hotmail.com (J. Liu).

0925-8388/$ – see front matter © 2007 Elsevier B.V. All rights reserved.
doi:10.1016/j.jallcom.2007.10.055

process was investigated. The effects of SiC content on the mechanical and thermal properties of SiC/Al composites were also studied.

2. Experimental

W28 yellow-green SiC powders in abrasive grade were used as the starting material and W10 super-pure graphite powders were used as pore-forming agents. The weight ratio of graphite and SiC powders initially taken was 0:100, 8:92 and 20:80 respectively. The powder mixtures added with 1 wt% stearic zinc as lubricant and water solution of 20 wt% polyvinyl alcohol as adhesive were ball-milled in tumbling box for 12 h. After drying in atmosphere for 12 h respectively, the mixtures were uniaxially pressed into wafer specimens of ϕ 10 mm × 5 mm and rectangular specimens of 5 mm × 5 mm × 40 mm under 100 MPa pressure using a stainless steel die. The following oxidation bonding process for the specimens was carried out in a box furnace at 1373 K for 3 h. SiC preforms bonded by SiO_2 film derived from the oxidation of SiC powders were obtained as Graphite, lubricate and adhesive were all burned out. The pressureless infiltration of liquid $AlSi_7Mg$ alloy into SiC preforms using magnesium as wetting agent was carried out in a tube resistance furnace filled constantly with high purity nitrogen gas in the whole process. After SiC preforms soaked above liquid Al alloy at 1173 K for 2 h, the specimens cooled down with furnace to room temperature. Since the infiltrated SiC preforms adhered firmly to the alloy, they had to be re-heated in crucible furnace to take the samples out by using crucible clamp. SiC/Al composites were finally achieved after alloy remains on its surface being filed off.

Since the shape keeps very well during the whole procedure, the density for porous SiC preforms was examined by a geometry method. The relative density of SiC/Al composites was calculated according to the following formula:

$$\theta = \frac{\rho_A}{V_{SiC}\rho_{SiC} + V_{Al}\rho_{Al}} \times 100 \quad (1)$$

where θ is the relative density, ρ_A is the density of SiC/Al composites measured by the Archimedes' principle, ρ_{SiC} and ρ_{A1} are the theoretical densities of SiC and aluminum alloy respectively ($\rho_{SiC} = 3.2\ g/cm^3$, $\rho_{A1} = 2.7\ g/cm^3$), V_{SiC} and V_{A1} are the volume fractions for SiC and aluminum alloy in the composite respectively.

The fractographs of SiC preforms were taken using X-650 scanning electron microscopy (SEM) and the ingredient of the samples was examined by XRD analysis. The microscopic structures of SiC/Al composites were observed by metallography technique. The pore size distribution of SiC preforms was determined by Poremastr GT-60 mercury porosimetry. The flexural strength and elastic modulus of SiC/Al composites were measured by a three-point bending at room temperature on an AG-25TA universal electron testing instrument. CTE was measured from room temperature to 373 K on a DIL 402C Dilatometer at 5 K min^{-1}. Thermal diffusion coefficient was measured using TC-7000H laser thermal diffusion instrument. TC can be calculated according to the following formula:

$$\lambda = 418.6\alpha C_p \rho \quad (2)$$

where α, C_p, ρ and λ are thermal diffusion coefficient, specific heat, density and TC for SiC/Al composites respectively.

3. Results and discussion

The sintered SiC preforms only has SiC and SiO_2 in it according to the XRD patterns shown in Fig. 1. SiO_2 is derived from the oxidation of SiC particles at 1373 K. Adhesive and lubricant were all eliminated by oxidation during the sintering process. Fig. 2 shows the fractograph of sintered SiC preforms. It was found that SiC particles bonded to each other by SiO_2 films on their surface to form a porous skeleton which has enough strength to maintain its shape in succeeding infiltration process. Fig. 3 shows the pore distribution of sintered SiC preforms,

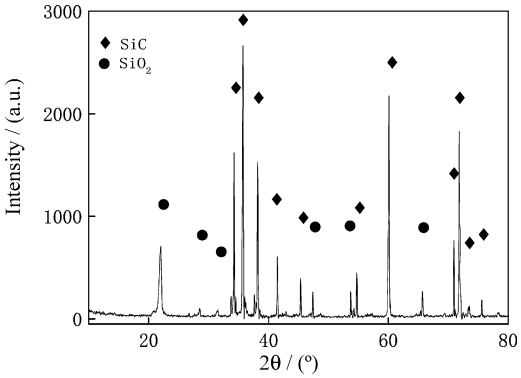

Fig. 1. XRD patterns of sintered SiC preforms.

which indicates that pores are all connected mutually to form an open pore-net. Two peaks existing in the curve shows that there are two type pores among SiC particles. The first type pore with size ranging from 0.2 to 6 μm is the clearance between adjacent SiC particles and the second with size about 9 μm is the void left by a graphite particle after it burned out. Since there are no remarkable difference in density and particle size between graphite and SiC, Graphite particles distribute evenly in the mixture, which led the second type pore distributes evenly too.

The infiltrated samples containing liquid aluminum alloy inside can be easily taken out from liquid metal bath in atmosphere by clamp and the composite keeps its shape very well. As liquid aluminum alloy cannot provide strength for the sample, a conclusion can be made that SiC filler constructs a three-dimension continuous phase, which attributes to silicon dioxide film on the surface of SiC powder. The XRD analysis of the infiltrated sample, as shown in Fig. 4, reveals that a few new phases, such as MgO, $MgAl_2O_4$ and Mg_2Si, appear during the

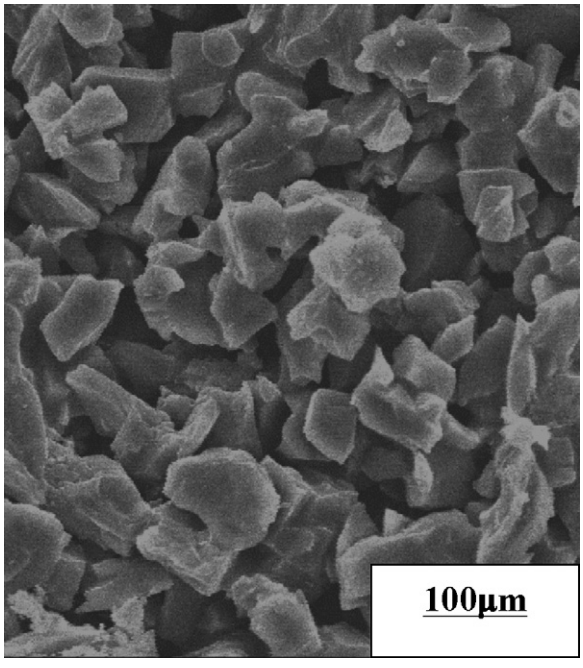

Fig. 2. Scanning electron fractograph of SiC preforms.

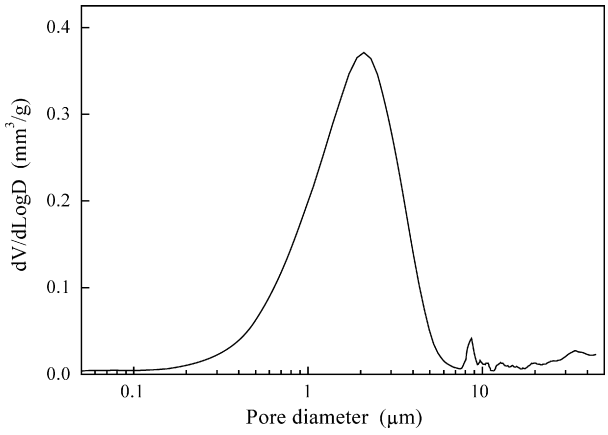

Fig. 3. Pore size distribution in SiC preforms.

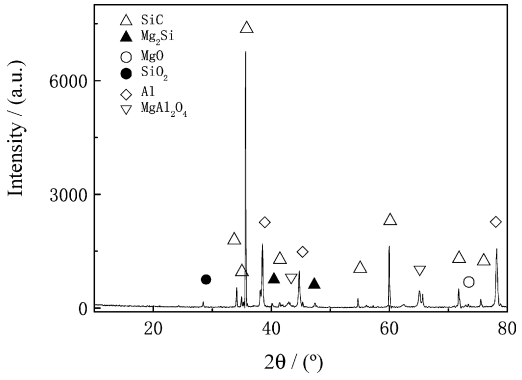

Fig. 4. XRD patterns of SiC/Al composites.

infiltration process. SiC preforms not only has open pore-net for liquid metal penetrating in, but also provides SiO_2 film as a good initial interface for liquid–solid reactions listed as below [18]:

$$SiO_2(s) + 2[Mg] = 2MgO(s) + [Si] \quad (3)$$

$$2SiO_2(s) + Al(l) + (1/2)[Mg] = (1/2)MgAl_2O_4(s) + [Si] \quad (4)$$

$$[Si] + 2[Mg] = Mg_2Si \quad (5)$$

Table 1
The evolution of density and dimension for samples during the whole process

Graphite content (wt%)	0	8%	20%
Relative density of SiC preforms	62%	52%	39%
Percent expansion of sintered SiC preforms	2.40%	3.60%	4.20%
Apparent density measured for SiC/Al composites (g/cm^3)	2.98	2.95	2.88
Relative density of SiC/Al composites	99.0%	99.6%	99.5%
Dimension change for SiC preforms infiltrated	(0.5)	(0.5)	(0.5)

These reactions remarkably decrease the liquid–solid interface energy, which is beneficial to improve wettability of the two phases and the spontaneous infiltration of liquid metal into porous SiC skeleton [19].

Fig. 5 shows the metallographic photographs for SiC/Al composites with different SiC volume fractions. Fig. 4(a)–(c) shows the microstructures for 62 vol.% SiC/Al, 52 vol.% SiC/Al and 39 vol.% SiC/Al composites respectively. It was found that SiC particles (bright grains) with clear edges and corners which shows that they keep their original shape very well due to the protection of SiO_2 film on its surface. As the abrasive resistance of SiC filler surpasses decisively that of Al alloy, SiC powders stick up gradually from Al alloy matrix during the whetting and polishing process to form a new and slick friction surface with stronger glistening than that of Al alloy matrix below it. As liquid Al alloy infiltrated into the preforms was divided by SiC skeleton into trivial branches, the growth of crystal of metal matrix was restrained seriously resulting in a fine crystal grain of metal matrix. The fining of crystal grains is beneficial to the strength of SiC/Al composites.

Variations of density and dimension for samples during the fabrication process were summarized in Table 1. Both SiC preforms with different relative density and SiC/Al composites with different SiC volume fraction ranging from 62% to 39% were obtained by modulating graphite fraction in initial mixture of powders ranging from 0 to 20 wt%. The relative densities of three groups of SiC/Al composites were all above 99.0% which indicates that near completely dense SiC/Al composites were achieved by the spontaneous infiltration of liquid Al

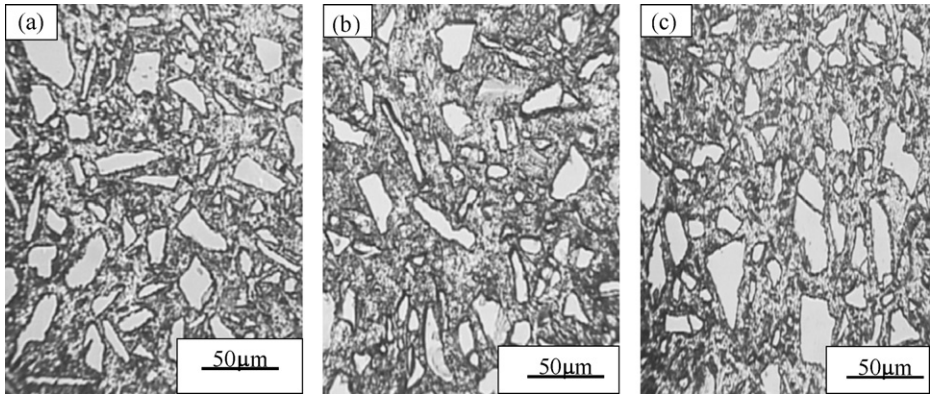

Fig. 5. Microstructure of SiC/Al composites: (a) 62 vol.% SiC/Al; (b) 52 vol.% SiC/Al; (c) 39 vol% SiC/A.

Table 2
Mechanical and thermal properties of SiC/Al composites

	Bending strength (MPa)	Elastic modulus (GPa)	TC ($W\,m^{-1}\,K^{-1}$)	CTE ($\times 10^{-6}\,K^{-1}$)
39% SiC/Al	374	147	146	10.5
52% SiC/Al	381	151	136	9.24
62% SiC/Al	366	158	118	8.45

alloy into porous SiC preforms enhanced by adding magnesium.

The dimension change of samples during the fabrication process could have significant effect on near-net-shape routine for SiC/Al composites. It was found from Table 1 that the dimension change mainly happened in the process of preparation of SiC preforms. There was no change in shape and dimension for SiC preforms during the pressureless infiltration process. The measurement value error for infiltrated samples is mainly ascribed to the oxidation of liquid metal on the surface of sample as it remelted in air. Formation of SiO_2 film on SiC surface during oxidation bonding could lead to a little expansion for the preforms. The percent expansion of SiC preforms increased from 2.4% to 4.4% with the increase of graphite fraction from 0% to 20%. Nevertheless, the expansion would not cause the preforms to deform, the tolerance for products of SiC/Al composite could be controlled accurately to achieve near-net-shape by careful mould designing to fit the sintering process of SiC preforms.

The mechanical and thermal properties of SiC/Al composites were summarized in Table 2. The flexure strengths of composites are all above 360 MPa, comparing to 280 MPa for casting $AlSi_7Mg$ shows a significant reinforcement of SiC filler on the strength of metal matrix, which is ascribed to the good wettability of interface and the formation of ceramic–metal interface bonding. The increase of strength does not have a linear relationship with the increasing SiC volume fraction. Exorbitant SiC content makes the composites brittle, resulting in the decrease of strength. In contrast, the improvement of elastic modulus for SiC/Al composites with increasing SiC content is more significant which are all above 140 GPa. The elastic modulus increases linearly with increasing SiC volume fraction. Having a low density, only about 3 g/cm^3, the SiC/Al composite is a new material with high specific strength and elastic modulus.

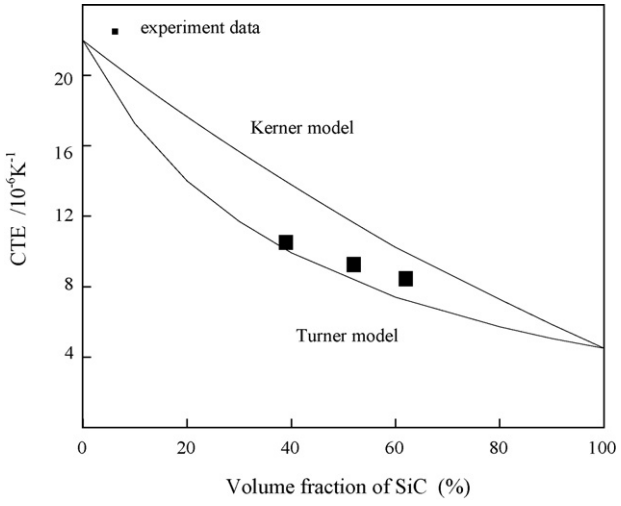

Fig. 6. CTEs of SiC/Al via SiC volume fraction.

The mean CTEs ranging from room temperature to 373 K of three kinds of SiC/Al composites with different SiC contents are $10.5 \times 10^{-6}\,K^{-1}$ (39 vol.% SiC), $9.24 \times 10^{-6}\,K^{-1}$ (52 vol.% SiC) and $8.45 \times 10^{-6}\,K^{-1}$ (62 vol% SiC) respectively, matching well to that of semiconductor materials including GaAs and Si, which enable them to be used as electronic package materials. As a result of interaction of the two co-continuous phases, the expansion behavior of SiC/Al composites trends complex. Since CTE of SiC is much lower than that of metal, the enormous difference of CTEs between two phases induces strong thermal stresses when temperature changes. On the assumption of only stresses existing in the interface, thermal expansion model for composites advanced by Turner [20] could be expressed as following:

$$\alpha_c = \frac{\alpha_m K_m V_m + \alpha_p K_p V_p}{K_m V_m + K_p V_p} \tag{6}$$

where α, K and V are CTE, bulk elastic modulus and volume fraction respectively. C, m and p subscripts represent composites, metal matrix and SiC reinforcement respectively.

Considering stress and shear stress both exist in the interface, a mended model represented by Kerner [21] is shown as following:

$$\alpha_c = \alpha_m V_m + \alpha_p V_p + V_p V_m(\alpha_p - \alpha_m) \times \frac{K_p - K_m}{K_m V_m + K_p V_p + 3K_p K_m/4G_m} \tag{7}$$

where G_m is the shear modulus for metal matrix.

Comparison of the CTEs experiment data with the two models above was shown in Fig. 6. It was found that the experiment data agreed better with Turner's model. As Al alloy was divided by three dimensional co-continuous SiC skeleton into exiguous branches without pores existing in the interface, free shearing deformation of metal matrix was inhibited severely by rigid SiC skeleton, which led to harmonious deformation of metal matrix with SiC filler.

Because Al alloy has much higher TC than SiC, which has many impurities in it, the TC of metal matrix decreased with increasing SiC filler added in, and TC depressed further more when plenty of metal–ceramic interface bonding formed in the composites. TCs at room temperature for SiC/Al composites with different SiC contents were shown in Table 2. It was found that TC decreased monotonously with increasing SiC content, ranging from 118 to 146 $W\,m^{-1}\,K^{-1}$, much higher than that of Kovar alloy (17 $W\,m^{-1}\,K^{-1}$) and slightly lower than that of

W–15Cu alloy (ranging from 160 to 190 $W\,m^{-1}\,K^{-1}$) [22]. As its density is less than one fifth of that of W–15Cu alloy, Al/SiC composite has tremendous potential to substitute W–Cu alloys used in the electronic heat package.

4. Summary and conclusion

SiC preforms with different Porosity were obtained by the oxidation process, which used W28 yellow-green SiC powders in abrasive grade as the starting material and W10 super-pure graphite powders as the pore-forming agents. There are two types of pores in SiC preforms. The first type is the clearance between adjacent SiC particles; the second is the voids left by burned out graphite particles. Pores were all connected mutually to form an open pore-net for liquid $AlSi_7Mg$ infiltrating in. Liquid Al alloy spontaneously infiltrated into porous SiC preforms enhanced by interface reaction between solid SiO_2 film derived from the oxidation of SiC and magnesium in liquid Al alloy. The mean thermal expansion coefficient of sintered SiC preforms increased from 2.4% to 4.4% with the increase of graphite volume fraction from 0% to 20%. Nevertheless, the expansion did not cause the preforms to deform. There was no change in shape and dimension for SiC preforms during the pressureless infiltration process. The tolerance for products of SiC/Al composites could be accurately controlled by careful mould designing to achieve near-net-shape after sintering. As SiC volume fraction increased from 39% to 62% with decreasing graphite content from 20% to 0% in initial mixed powders, the thermal conductivity of SiC/Al composites with bending strength beyond 360 MPa and elastic modulus beyond 140 GPa decreased from 146 to 118 $W\,m^{-1}\,K^{-1}$ at room temperature. In corresponding, the mean linear coefficient of thermal expansion from room temperature to 373 K decreased from 10×10^{-6} to $7.69 \times 10^{-6}\,K^{-1}$, agreeing better with Turner's model.

Acknowledgements

This work has been financially supported by Innovation Groups Foundation (103-037016) and Development Foundation (103-037508) of Hefei University of Technology, China.

References

[1] C. Zweben, JOM 44 (1992) 15–23.
[2] S. Elomri, R. Bouhili, C.S. Marchi, A. Mortensen, D.J. Lloyd, J. Mater. Sci. 32 (1997) 2131–2140.
[3] A.L. Geiger, M. Jackson, Adv. Mater. Proc. 136 (1989) 23–28.
[4] E.M. Klier, A. Mortensen, J.A. Cornie, M.C. Flemings, J. Mater. Sci. 26 (1991) 2519–2526.
[5] M. Hunt, Mater. Eng. 108 (1991) 24–25.
[6] J.L. Bugeau, Proceedings of the IEEE MTT-S International Microwave Symposium, 1995, pp. 1575–1578.
[7] Q. Huang, Y.P. Jin, M.Y. Gu, Intro. Mater. 9 (2002) 18–19 (in Chinese).
[8] M.I. Pech-Canul, R.N. Katz, M.M. Makhlouf, J. Mater. Process. Technol. 108 (2000) 68–77.
[9] R. Arpon, J.M. Molina, R.A. Saravanan, et al., Acta Mater. 51 (2003) 3145–3152.
[10] A. Zulfia, R.J. Hand, J. Mater. Sci. 37 (2002) 955–961.
[11] T.U. WC, F. Lange, J. Am. Ceram. Soc. 78 (1995) 3277–3282.
[12] X.M. Xi, X.F. Yang, J. Am. Ceram. Soc. 79 (1996) 102–108.
[13] V.M. Kevorkijan, Compos. Sci. Technol. 59 (1999) 683–686.
[14] M. Rodríguez-Reyes, M.I. Pech-Canul, E.E. Parras-Medécigo, A. Gorokhovsky, Mater. Lett. 57 (2003) 2081–2089.
[15] X.M. Xi, L.M. Xiao, X.F. Yang, J. Mater. Res. 11 (1996) 1037–1044.
[16] J.M. Chiou, D.D.L. Chung, J. Mater. Sci. 28 (1993) 1435–1446.
[17] J.M. Chiou, D.D.L. Chung, J. Mater. Sci. 28 (1993) 1447–1470.
[18] P.L. Rantnaaparkhi, J.M. Howe, Metall. Mater. Trans. A 25 (1994) 617–627.
[19] H. Kaneda, T. Choh, J. Mater. Sci. 32 (1995) 1469–1472.
[20] P.S. Turner, J. Res. NBS 37 (1946) 239.
[21] E.H. Kerner, Proc. Phys. Soc. 69 (1963) 802.
[22] Q. Zhang, D.L. Sun, G.H. Wu, Mater. Sci. Technol. 4 (2000) 66–70 (in Chinese).